https://doi.org/10.5194/cp-2021-111
Preprint. Discussion started: 7 September 2021

Climate of the Past Discussions

The De Long Trough: defining the mineralogical signature of the East Siberian Ice Sheet

Raisa Alatarvas[1], Matthew O'Regan[2], Kari Strand[1]

[1]Oulu Mining School, University of Oulu, Oulu, 90570, Finland

[2]Department of Geological Sciences, Stockholm University, Stockholm, 106 91, Sweden

Correspondence to: Raisa Alatarvas (raisa.alatarvas@oulu.fi)

Abstract. The Arctic's glacial history has classically been interpreted from marine records in terms of the fluctuations of the Eurasian and North American ice sheets. However, the existence, size, and timing of the East Siberian Ice Sheet (ESIS) remains highly uncertain. A recently discovered glacially scoured cross-shelf trough extending to the edge of the continental shelf north of the De Long Islands has provided additional evidence that glacial ice existed on parts of the East Siberian Sea (ESS) during previous glacial periods (MIS 6 and 4). This study concentrates on defining the mineralogical signature and dynamics of the ESIS. Sediment materials from the East Siberian shelf and slope were collected during the 2014 SWERUS-C3 expedition. The cores studied are 20-GC1 from the East Siberian shelf, 23-GC1 and 24-GC1 from the De Long Trough (DLT), and 29-GC1 from the southern Lomonosov Ridge (LR). Heavy mineral assemblages were used to identify prominent parent rocks in hinterland and other sediment source areas. The parent rocks areas include major eastern Siberian geological provinces such as the Omolon massif, the Chukotka Fold Belt, the Verkhoyansk Fold Belt, and possibly the Okhotsk–Chukotka Volcanic Belt. The primary riverine sources for the ESS sediments are the Indigirka and Kolyma rivers, which material then was glacially eroded and re-deposited in the DLT. The higher abundances of hornblendes in the heavy mineral assemblages may indicate ESS paleovalley of the Indigirka river as a major pathway of sediments, while the Kolyma river paleovalley pathway relates to a higher share of pyroxenes and epidote. Mineralogical signature in the DLT diamicts, consisting predominantly of amphiboles and pyroxenes with minor content of garnet and epidote, show clear delivery from the eastern sector of the ESIS. Although the physical properties of the DLT basal diamict closely resemble a pervasive diamict unit recovered across the southern LR, their source material is slightly different according to their heavy mineral content. Assemblages with elevated amphibole and garnet content, along with higher titanite and ilmenite content from core 29-GC1 from the southern LR emphasise the Verkhoyansk Fold Belt as a possible source. This suggests that glacial ice not only grew out from the East Siberian shelf, but also from the New Siberian Islands and westerly sources due to the dynamics in the ice flow and deposition. An increase in the iron oxides in the sediments overlying the diamicts relates to the deglaciation cycle of the ESIS when the central plateau, or at least the shoreline and river discharge region, were possibly free from ice, and the reworking as well as enrichment of iron oxides was possible. This indicates sea-ice rather than iceberg transport for the present distal shelf sediments.

Introduction

The existence, timing and extent of ice sheets during the Pleistocene glaciations on the Siberian continental shelf of the East Siberian Sea is still largely undetermined. The sparse geophysical and marine geological data obtained from this area are highly

https://doi.org/10.5194/cp-2021-111
Preprint. Discussion started: 7 September 2021

important in defining the glacial history of the region and its relationship to the wider Eurasian Arctic glaciations. Regardless of the lack of characteristic glacial features, previous studies have suggested the existence of ice sheets over parts of the East Siberian continental shelf during the larger Pleistocene glaciations following the mid-Pleistocene transition (Colleoni et al., 2016; Niessen et al., 2013), the Saalian (Marine Isotope Stage 6) (Jakobsson et al., 2016).

This study concentrates on defining the mineralogical signature and distribution of the ESIS from marine sediments from the East Siberian shelf and slope, especially from a glacial trough and related trough mouth fan setting. Information about the glacial history of a continental margin can be obtained from the temporal evolution of trough mouth fan system (Stein, 2008). Studied sediment cores were collected during the SWERUS-C3 2014 expedition (SWERUS-C3: Swedish – Russian – US Arctic Ocean Investigation of Climate-Cryosphere-Carbon Interactions) from the East Siberian continental shelf and slope. The overreaching aim is to evaluate the heavy mineral composition to see if there is a unique mineralogical signature in diamict samples from the newly discovered DLT that can be used for far field reconstructions of ice sheet activity on the east Siberian margin. The mineralogical components and mineral-geochemical characteristics of these samples provide interpretative data for reconstruction of potential source areas and pathways for glacially entrained sediments. The relevance of this work is the utilization of heavy mineral assemblages of the East Siberian shelf and slope sediments as provenance tracers. Examination of heavy minerals in the coarse fraction can be used in estimation of provenance and source areas, and plausible transport mechanisms. The majority of rock types and their component minerals are presumably represented in the sand fraction in the straightforward case of subglacial erosion, transport and deposition (Licht and Hemming, 2017). Provenance information can be derived from individual sand-size heavy mineral grains or populations of grains and identification of mineral assemblages indicating certain metamorphic and igneous source terranes provide a key provenance information.

1 Introduction

The existence, timing and extent of ice sheets during the Pleistocene glaciations on the Siberian continental shelf of the East Siberian Sea is still largely undetermined. The sparse geophysical and marine geological data obtained from this area are highly important in defining the glacial history of the region and its relationship to the wider Eurasian Arctic glaciations. Regardless of the lack of characteristic glacial features, previous studies have suggested the existence of ice sheets over parts of the East Siberian continental shelf during the larger Pleistocene glaciations following the mid-Pleistocene transition (Colleoni et al., 2016; Niessen et al., 2013), the Saalian (Marine Isotope Stage 6) (Jakobsson et al., 2016).

This study concentrates on defining the mineralogical signature and distribution of the ESIS from marine sediments from the East Siberian shelf and slope, especially from a glacial trough and related trough mouth fan setting. Information about the glacial history of a continental margin can be obtained from the temporal evolution of trough mouth fan system (Stein, 2008). Studied sediment cores were collected during the SWERUS-C3 2014 expedition (SWERUS-C3: Swedish – Russian – US Arctic Ocean Investigation of Climate-Cryosphere-Carbon Interactions) from the East Siberian continental shelf and slope. The overreaching aim is to evaluate the heavy mineral composition to see if there is a unique mineralogical signature in diamict samples from the newly discovered DLT that can be used for far field reconstructions of ice sheet activity on the east Siberian margin. The mineralogical components and mineral-geochemical characteristics of these samples provide interpretative data for reconstruction of potential source areas and pathways for glacially entrained sediments. The relevance of this work is the utilization of heavy mineral assemblages of the East Siberian shelf and slope sediments as provenance tracers. Examination of heavy minerals in the coarse fraction can be used in estimation of provenance and source areas, and plausible transport

https://doi.org/10.5194/cp-2021-111
Preprint. Discussion started: 7 September 2021

Climate of the Past Discussions

mechanisms. The majority of rock types and their component minerals are presumably represented in the sand fraction in the straightforward case of subglacial erosion, transport and deposition (Licht and Hemming, 2017). Provenance information can be derived from individual sand-size heavy mineral grains or populations of grains and identification of mineral assemblages indicating certain metamorphic and igneous source terranes provide a key provenance information.

2 Regional and geological setting

2.1 The East Siberian Sea and Shelf

The East Siberian Arctic Shelf extends ~2,500 km from the eastern Taimyr Peninsula coast from the ESS and Laptev Sea to the Russia and US marine border in the Chukchi Sea, containing the New Siberian and De Long Archipelagos island groups, and Wrangel Island (Drachev et al., 2018). The East Siberian continental shelf extends over the North American Plate and the East Siberian Platform, and it is covered by the ESS and the Laptev Sea. The shelf is composed of younger crust of the Late Mesozoic fold belts overlain with Late Mesozoic and Cenozoic siliciclastic sediments (Drachev et al., 2010). The East Siberian Sea Basin is filled with siliciclastic sediments with inferred stratigarphic range of Late Cretaceous to Quaternary age (Drachev et al., 2010).

The ESS is a relatively shallow sea. In the course of the larger glaciations following the mid-Pleistocene transition after 1.5 Ma, and during the sea level low stand of the Last Glacial Maximum (LGM), the region was most likely exposed due to most of the region having a depth of <120 m (Lambeck et al., 2014; Rohling et al., 2014). According to Klemann et al. (2015), througout glacial periods, the ESS was largely exposed due to the global mean sea level being more than 100 m lower than its present value. During regressive and transgressive cycles, the shallowness of the shelf also might have led to erosion of submarine glacial landforms which are an indication of the presence of ice sheets (Dowdeswell et al., 2016; O'Regan et al., 2017).

In the east, the continental slope of the ESS connects to the Mendeleev Ridge and Makarov Basin (O'Regan et al., 2016), with the latter adjoining the LR by extended continental crust (Jokat and Ickrath, 2015). The LR is underwater ridge of continental crust expanding from the northern Greenland shelf, through the North Pole, to the central Siberian continental shelf, dividing the Arctic into the Eurasian and Amerasian basins (e.g., Kristoffersen et al., 1990; Cochran et al., 2006).

2.2 Glacial cross-shelf troughs and trough mouth fans

The existence of glacially excavated cross-shelf troughs (CSTs) indicate fast-streaming glacial ice areas on formerly glaciated margins (Batchelor and Dowdeswell, 2014). Bathymetrically prominent trough mouth fans (TMFs) are formed from large volumes of subglacial sediment discharging seaward of the shelf break onto the slope in front of CSTs (Ó Cofaigh et al., 2003; Batchelor and Dowdeswell, 2014). TMFs are stacked glaciogenic debris flows interbedded with open-water or ice-distal marine sediments formed by fast-streaming ice transporting large volumes of subglacial sediments to the shelf break (Laberg and Vorren, 1995; Elverhøi et al., 1997; Dowdeswell and Ó Cofaigh, 2002; Batchelor and Dowdeswell, 2014). Ó Cofaigh et al. (2003) concluded that the ideal conditions for TMF formation include a tectonically passive marginal setting; wide continental shelf; deformable, readily erodible sediments on the adjacent continental shelf; high rates of sediment delivery to the shelf edge; and a low (<1°) slope gradient. According to Batchelor and Dowdeswell (2014) the formation of TMFs is more prominent in front of CSTs with recurrent ice stream activity through several glacial cycles, and where sediment is transported to comparatively shallow continental slopes.

https://doi.org/10.5194/cp-2021-111
Preprint. Discussion started: 7 September 2021

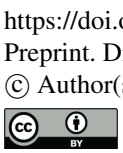

Climate of the Past Discussions
Open Access
EGU

Seismic and bathymetric data illustrate many glacially excavated troughs which discharged ice into the Arctic Ocean (Fig. 1) (Batchelor and Dowdeswell, 2014). Many of these troughs trace back in the direction of the center of former ice sheets, or back into branching fjords on adjoining landmasses (Batchelor and Dowdeswell, 2014; Jakobsson et al., 2016). Prior to the SWERUS-C3 2014 expedition (e.g. Jakobsson et al., 2016; O'Regan et al., 2017) no evidence for CSTs existed on the shallow shelf of the ESS. The DLT is the first glacial trough reported on the outer margin of the East Siberian shelf and is located north from the De Long and New Siberian Islands (Fig. 1) (O'Regan et al. 2017). The area interpreted as a TMF in front of the DLT totals 6540 km^2, with an average slope angle of 1.2, and thickness of the glacio-genic debris flow sequence of more than 65 m (O'Regan et al. 2017).

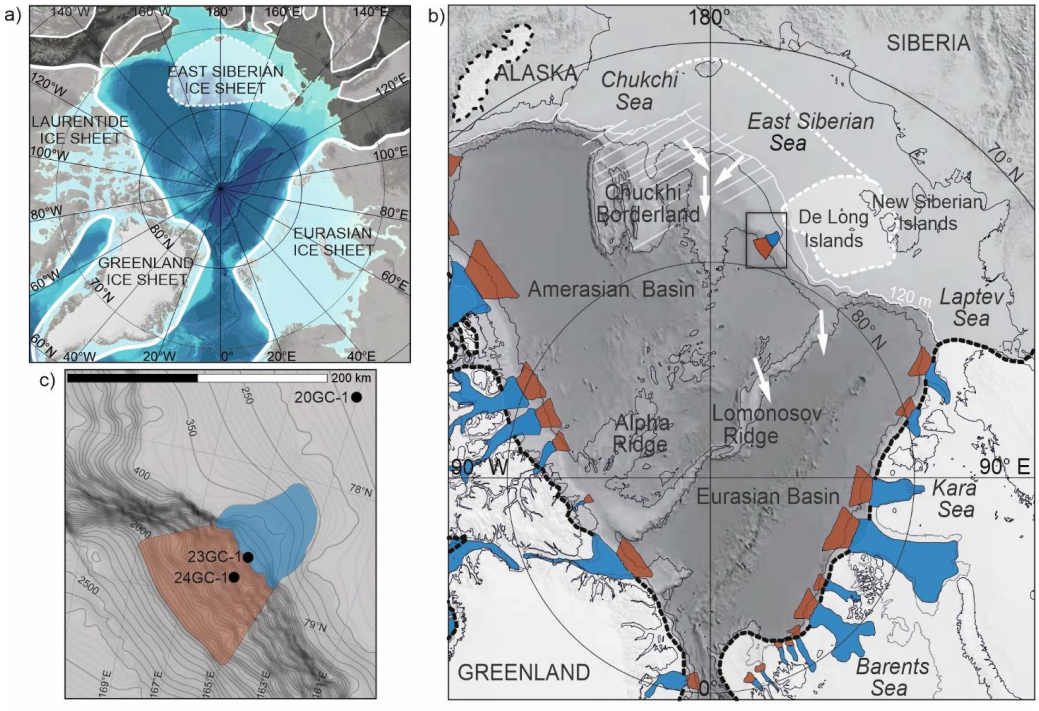

Figure 1: a) Quaternary ice sheets in the Arctic according to Jakobsson et al. (2010). Proposed maximum extent of the East Siberian Ice Sheet, and LGM ice in Siberia and Alaska redrawn from Niessen et al. (2013). Base map from the International Bathymetric Chart of the Arctic Ocean (IBCAO) by Jakobsson et al. (2012). b) The extent of Quaternary glaciations in the Arctic region is shown by black and white dashed lines according to Jakobsson et al. (2014). The possible extent of exposed land during the global eustatic low stand of the LGM is highlighted with the 120 m isobath across the Chukchi and East Siberian seas (O'Regan et al., 2017). White arrows indicate the direction of ice flow by Jakobsson et al. (2016) and glacial extent around the De Long Islands redrawn from Basilyan et al. (2008), respectively. Glacially excavated cross-shelf troughs (blue) and trough mouth fans (brown) are according to Batchelor and Dowdeswell (2014), and the single trough (De Long Trough) on the East Siberian shelf by O'Regan et al. (2017). Black rectangle marks the location of the map shown in c. Original figure by O'Regan et al. (2017). c) Insert figure showing the locations of studied cores 20-GC1, 23-GC1 and 24-GC1, as well as brown and blue areas illustrate the constraints of the De Long glacial trough and trough mouth fan deposits (O'Regan et al., 2017). Original figure by O'Regan et al. (2017).

The occurence and direction of glaciogenic features and sedimentary deposits on the lower slope of the ESS, on the seafloor in the Amerasian Basin, and on the crest of shallower plateaus and ridges, offer evidence for glacial ice on the Siberian continental shelf (Niessen et al., 2013; Jakobsson et al., 2016). The direction of streamlined glacial lineations on the base of the East Siberian continental slope, Arlis Plateau seabeds (Fig. 1) indicate ice flow from the East Siberian shelf (Niessen et al., 2013; Jakobsson et al., 2016). Grounded glacial ice flowing from the East Siberian shelf is also indicated by glacial lineations

https://doi.org/10.5194/cp-2021-111
Preprint. Discussion started: 7 September 2021

Climate of the Past Discussions
Open Access
EGU

on an ice-scoured crest of the southern LR, along with a steep lee side towards the Amundsen Basin and a lightly sloping stoss side facing the Makarov Basin (Jakobsson et al., 2016).

3 Materials and methods

The samples studied in this paper are from four sediment cores which were collected during Leg 2 of the SWERUS-C3 2014 expedition on the Ice Breaker *Oden* that departed 21 August from Barrow, Alaska and ended 3 October in Tromsø, Norway (Fig. 2). Samples are from cores 20-GC1, 23-GC1, 24-GC1 and 29-GC1, which were collected from various locations and water depths (Table 1).

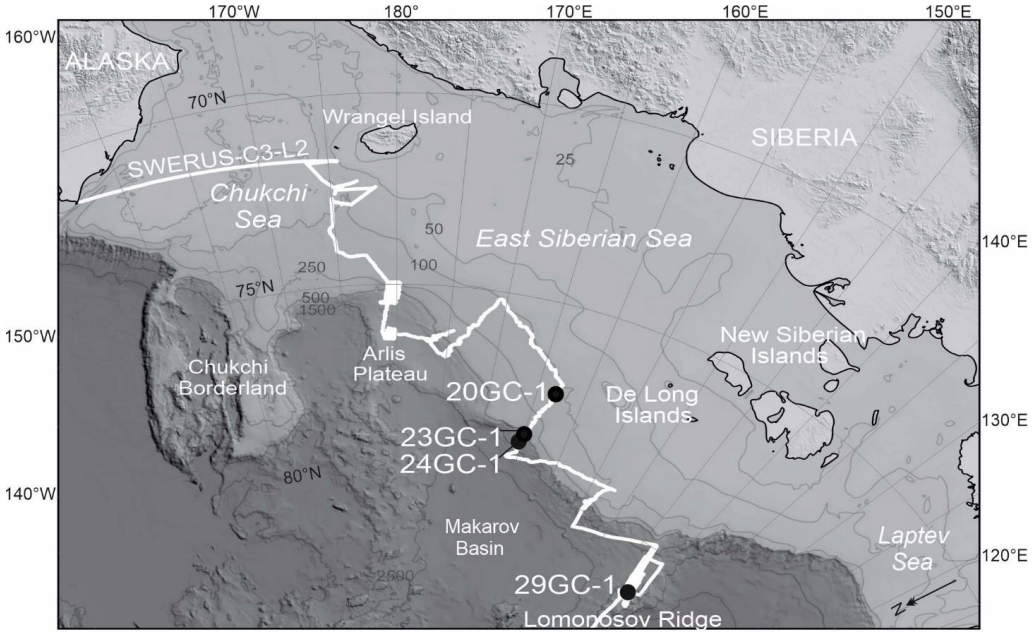

Figure 2: Map showing the locations of studied cores 20-GC1, 23-GC1, 24GC-1 and 29-GC1, and the route of Leg 2 of the SWERUS-C3 2014 expedition (white line). Original figure by O'Regan et al. (2017).

Table 1: Locations, lengths, and water depths of the cores studied. Data from O'Regan et al. (2017) and the SWERUS cruise report (2014).

Core	Water depth	Length (m)	Latitude	Longitude	Location
20–GC1	115	0.83	77°21.5' N	163°2.0' E	East Siberian Shelf
23–GC1	508	4.06	78°39.7' N	165°0.9' E	De Long Trough
24–GC1	964	4.05	78°47.8' N	165°22.0' E	De Long Trough
29–GC1	824	4.66	81°17.9' N	141°46.9' E	Southern Lomonosov Ridge

3.1 Physical properties and geophysical mapping

The cores studied were collected using a gravity corer (GC). The unsplit sediment cores were logged shipboard on a Multi-Sensor Core Logger (MSCL). Magnetic susceptibility, bulk density, and compressional-wave velocity (*p* wave) were measured at a downcore resolution of 1 cm. The cores were split, described, and imaged shipboard. Shore-based measurements on the cores were done at the Department of Geological Sciences, Stockholm University. These included grain size and x-ray fluorescence (XRF) core scanning and additional magnetic susceptibility. Geophysical mapping methods during the expedition

https://doi.org/10.5194/cp-2021-111
Preprint. Discussion started: 7 September 2021

included multibeam bathymetry and sub-bottom profiles collected with Kongsberg EM 122 (12 kHz, 1° x 1°) multibeam echosounder hull and Kongsberg SBP 120 3° x 3° chirp sonar integrated with the multibeam in *IB Oden* (Jakobsson et al., 2016).

According to O'Regan et al. (2017) the sub-bottom stratigraphy from the shallow East Siberian shelf to the shelf break is divided into six acoustic units, and two of the studied cores (23-GC1 and 24-GC1) are divided into two sedimentary units A and B. The division and correlation between sedimentary units is based on grain size and physical properties data and incorporation of the Ca/Ti ratio from the XRF-scanning data. A short description of the units is presented here; further details are presented in O'Regan et al. (2017). Acoustic Unit (AU) 1 is a thin, discontinuous, and largely incoherent veneer of sediments interpreted as iceberg-scoured postglacial sediments that has a sharp basal contact on the shallow shelf (< 100-150 m). In deeper water depths the unit thickens and incorporate preglacial and glacial sediments reworked by the last glacial cycle sea level lowering. AU 2 is mainly horizontally layered or dipping and truncated reflection packages, which are interspersed with intervals of acoustically transparent material, and the unit is interpreted as outcropping sedimentary or bedrock strata with no knowledge of its age or composition. AU 3 is a coherent and laterally continuous acoustically layered sequence extending seaward of the shelf break and downslope to water depths of > 2000 meters below sea level (m b.s.l.). The base of AU 3 is defined by a hummocky reflector that overlies acoustically transparent AU's 4 and 5, which are interpreted as sub-glacially deposited sediments. The bases of these units are separated at the shelf break by a distinct acoustically transparent, wedge-shaped sediment package defined as AU 6, interpreted as either a mass wasting deposit or an ice-proximal fan. Core 20-GC1 sampled sediments from AU 1. Cores 23-GC1 and 24-GC1 penetrated to the base of the acoustically laminated AU 3. The acoustically laminated sediments are represented by sedimentary Unit A in the cores. These undisturbed sediments overlie the coarser-grained glacial diamict of sedimentary Unit B, which corresponds to AU 4. The base of core 20-GC1 has similar sedimentary characteristics to Unit B in 23-GC1 and 24-GC1, but it is not syndepositional.

3.2 Sediment cores and heavy mineral samples

A total of 17 samples were analyzed in this study (Table 2), and their location in relation to the sediment stratigraphy are illustrated using the digital images of the cores (Fig. 3). Two samples are from the 0.83 m long core 20-GC1, which was recovered in 115 m water depth from the East Siberian shelf, near the DLT. The core contains dark grey coarser-grained facies at its base and sediments with lower-density and susceptibility above 0.5 meters below sea floor (m b.s.f.). Two diamict samples are from the 4.06 m long core 23-GC1 which was recovered in water depth of 508 m and nine samples are from 4.05 m long core 24-GC1 recovered in water depth of 964 m from the DLT. The samples from core 24-GC1 also include surface sediments and other lithologies found between the seafloor and the diamict. These samples help define the mineralogy of the diamict in comparison to the overlying sediments from the last glacial cycle. Four samples are from core 29-GC1. The 4.66 m long core was recovered in 824 m water depth from the southern LR, and the core sampled acoustically stratified sediments deposited on top of the ice-scoured surface (Jakobsson et al., 2016). The base of this core represented now by three samples recovered a dark grey diamict whose mineral assemblage is compared to the DLT diamict samples.

https://doi.org/10.5194/cp-2021-111
Preprint. Discussion started: 7 September 2021

Climate of the Past Discussions
Open Access
EGU

Table 2: Depth, cm interval and description of the 17 studied samples from cores 20-GC1, 23-GC1, 24-GC1 and 29-GC1.

Sample	Core	Section	Depth	cm	Description	Location
1	20–GC1	CC	0.76	22-24	grey diamict	East Siberian shelf
2	20–GC1	CC	0.81	27-29	grey diamict	East Siberian shelf
3	23–GC1	3	3.66	108-110	grey diamict	De Long Trough
4	23–GC1	3	3.86	128-130	grey diamict	De Long Trough
5	24–GC1	1	0.04	3-5	dark brown clay	De Long Trough
6	24–GC1	1	0.53	52-54	light brown silty-clay	De Long Trough
7	24–GC1	1	0.99	98-100	olivegreen-grey silty clay	De Long Trough
8	24–GC1	2	1.53	47-49	olivegreen-grey silty clay	De Long Trough
9	24–GC1	2	2.09	104-106	light brown silty clay	De Long Trough
10	24–GC1	3	2.88	34-36	grey clay above diamict	De Long Trough
11	24–GC1	3	3.12	58-60	grey clay above diamict	De Long Trough
12	24–GC1	3	3.61	108-110	grey diamict	De Long Trough
13	24–GC1	3	3.77	122-124	grey diamict	De Long Trough
14	29–GC1	4	4.31	114-116	light brown silty clay	Southern Lomonosov Ridge
15	29–GC1	4	4.43	126-128	grey diamict	Southern Lomonosov Ridge
16	29–GC1	4	4.55	138-140	grey diamict	Southern Lomonosov Ridge
17	29–GC1	4	4.62	145-147	grey diamict	Southern Lomonosov Ridge

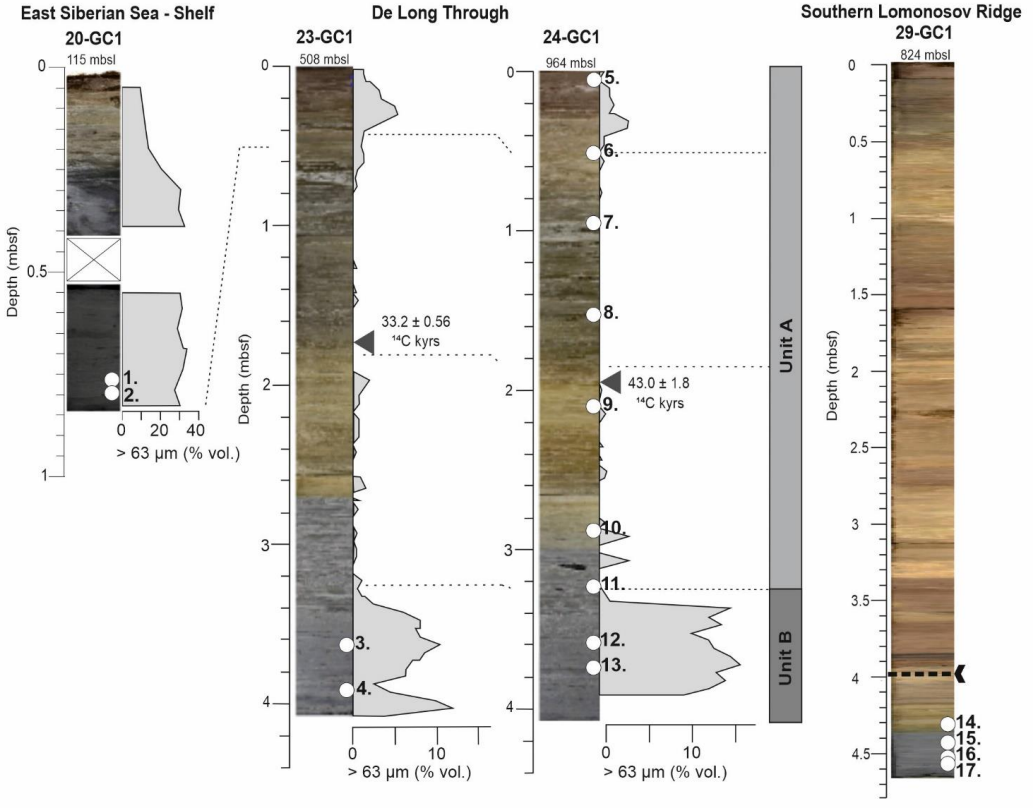

Figure 3: Digital images and locations of studied cores, including 17 sample points (white circles) (adapted from O'Regan et al., 2017). Stratigraphic correlation of the cores (dotted lines) and the division of sedimentary Units A and B are based on MSCL, XRF-scanning, grain size, digital images and radiocarbon dating results (O'Regan et al. 2017). Inferred MIS 5/6 transition (black dotted line) in core 29-GC1 from Jakobsson et al. (2016).

https://doi.org/10.5194/cp-2021-111
Preprint. Discussion started: 7 September 2021

Climate of the Past Discussions

3.3 Dating and chronology

Six radiocarbon ages were obtained from the core catcher of 20-GC1, and single range finding ages were obtained from both 23-GC1 and 24-GC1 (Cronin et al., 2017; O'Regan et al., 2017). Those accelerator mass spectrometry (AMS) radiocarbon measurements were performed at the Lund University Radiocarbon Dating Laboratory (Lu), Sweden, and at the National Ocean Sciences Accelerator Mass Spectrometry (NOSAMS) facility at Woods Hole Oceanographic Institution, Massachusetts on samples containing the planktonic foraminifer *Neogloboquadrina pachyderma*, mixed benthic foraminifera or mollusk shells. Radiocarbon dates from the lower part of core 20-GC1 outlined ages between ~ 13 and 11 ka and also indicate that the dense, deglacial, dark grey sediments in the lower part of 20-GC1 do not correlate to a similar lithology, that predates the LGM, at the base of cores 23-GC1 and 24-GC1 (Cronin et al., 2017). The sediments in the lower part of core 20-GC1 correlate with a thin, higher-susceptibility, and dense grey sediment sequence in the upper 0.5 m of cores 23-GC1 and 24-GC1 (Fig. 3). Radiocarbon dating from cores 23-GC1 (1.69–1.86 m b.s.f.) and 24-GC1 (1.92 m b.s.f.) give ages of 33 200 ± 560 and 43 000 ± 1800 ^{14}C years BP, and calibrated medium ages are 37 000 $\pm\frac{2600}{1300}$ and 46 300 $\frac{3500}{2600}$ cal years BP (O'Regan et al., 2017). Based on results from radiocarbon dating, the base of Unit A is older than ~ 50 cal kyr BP. Occurrence of the calcareous nannofossil *E. huxleyi* in core 23-GC1 at 2.28 m b.s.f. indicate, that the sediments in that point are younger than MIS 7/8 (Backman et al., 2009; O'Regan et al., 2017; O'Regan et al., 2020). O'Regan et al (2017) argued for an MIS 6 age for the basal diamict in 23-GC1 and 24-GC1, but acknowledged that it may have been deposiuted during a younger stadial in MIS 5 or 4. According to Jakobsson et al. (2016) Holocene age is indicated by calacareous nannofossils in the uppermost 5 cm of core 29-GC1, and an observation of *E. huxleyi* was made at 3.81 m b.s.f. The core correlates to a neighbouring core which base has been proposed an MIS 6 age by Stein et al., 2001. The inferred MIS 5/6 transition in core 29-GC1 is at ~ 4 m b.s.f. (Jakobsson et al., 2016).

3.4 Heavy mineral analysis

To clean the samples from adhering clays the samples were weighed and treated with 2 ml of dispersant solution, sodium pyrophosphate ($Na_4P_2O_7$) and distilled water. The samples were put in an ultrasonic cleaner for 30-45 minutes, and occasionally stirred with a glass rod. To separate the silt from the coarser fraction, the samples were wet-sieved into a fraction coarser than 63 µm and then dried and collected for heavy liquid separation. Nine samples had enough material for the heavy liquid separation with sodium heteropolytungstate (LST Fastfloat) with a density of 2.82 g/cm^3. The >63µm fraction was poured into a separating funnel consisting of heavy liquid. The mixture was shaken thoroughly and left to allow the heavy minerals to separate from the light minerals. After separation, the heavy fraction was drained onto a filter paper and cleansed with distilled water using a Büchner funnel for suction filtration. The filter paper with the heavy fraction was dried at 60 °C and the dry fraction collected. Heavy mineral separation was done for six samples with liquid nitrogen, following the method of Mange and Maurer (1992). Heavy mineral separation was not done for two samples due to the low amount of material. The heavy mineral samples for the electron microscope were prepared in the thin section laboratory at Oulu Mining School, University of Oulu.

The heavy mineral grains >63 µm from 17 samples were analyzed with Zeiss Ultra Plus Scanning Electron Microscope (SEM) at the Centre for Material Analysis, University of Oulu. Heavy mineral identification was done by using MinIdent-Win 3.0 computer program. The 18 analyzed elements Na, Mg, Al, Si, P, S, K, Ca, Ti, V, Cr, Fe, Cu, Zn, Zr, La, Ce, and Nd (expressed as oxides) were used in specification of the minerals.

https://doi.org/10.5194/cp-2021-111
Preprint. Discussion started: 7 September 2021

Climate of the Past Discussions
Open Access
EGU

4 Results

4.1 Sediment stratigraphy

Lithostratigraphic definition and stratigraphic correlation of the cores 20-GC1, 23-GC1 and 24-GC1 are based on digital images, MSCL, XRF-scanning, grain size and radiocarbon dating results by O'Regan et al. (2017) (Fig. 3). Core 20-GC1 was obtained from shallower shelf containing dark grey finer-grained deglacial sediments with coarser-grained facies at its base. The bases of 23-GC1 and 24-GC1 (sedimentary unit B) also contain a dark grey and poorly sorted sequence of coarser-grained sediments, which is interpreted as a diamict, and there is a less pronounced coarser-grained interval present in the upper 50 cm of these cores. Surface sediments and lithologies from the last glacial cycle found between the seafloor and the diamict in core 24-GC1 include dark and light brown clay, olive green-grey silty clay, and grey clay. The base of core 29-GC1 also has dark grey diamict sequence overlain by light brown silty clay.

4.2 Heavy minerals

The heavy minerals presented in this study are the major silicates including amphiboles, pyroxenes, epidote, garnets, micas, titanite and zircon, and other heavy minerals including Fe-oxides, ilmenite, other oxides (anatase, crichtonite, armalcolite), phosphates, sulphides (kieserite, voltaite) and others (vesuvianite, olivine, neptunite, chlorite). The abundance of each identified mineral is presented as a relative percentage of the total grains counted in each sample. Total amount of identified grains varies throughout the samples and the quantity of total grains (n) is low in a few samples due to scarce amount of grains >63μm and lack of heavy minerals.

The comparison of heavy mineral assemblages between different diamict samples and deglacial sediment samples can be considered after mineral identification based on geochemical compositions (Fig. 4). Especially important is to compare the LR diamict assemblages in core 29-GC1 (samples 15-17) with the diamict assemblages in the DLT samples from cores 23-GC1 and 24-GC1. Two interglacial samples from core 20-GC1 (1-2) are close to DLT and one light brown silty clay sample (14) overlays dark grey diamicts at the base of core 29-GC1 from the southern LR (Fig. 4). The heavy minerals assemblages of the samples from core 20-GC1 consists of major amphiboles (22–43%), pyroxenes (15%), epidote (7–11%), and minor garnets (3–14%), and titanite (~10%), with a distinct occurrence of zircon, Fe-oxides and ilmenite, along with other oxides, phosphates, and others with a concentration between 1 to 8%. In core 23-GC1 the heavy mineral assemblages consist mainly of amphiboles (24%), pyroxenes (~17%), and epidote (11–16%), and other minerals with a concentration varying from 1 to 11%. In core 24-GC1 amphiboles (33–39%), pyroxenes (17–21%), and epidote (7–17%) are also main contributors to the heavy mineral assemblages, whereas minor minerals are present in smaller amounts varying from 1 to 6%. Core 29-GC1 has the highest amphibole content varying between 33 and 50%. Pyroxenes (7–14%) and epidote (8–20%) content is relatively lower but are also the main contributors. The presence of minor minerals varies between 1 and 10%. There is a prominent increase in amphibole content in core 29-GC1 and a lower pyroxene content compared to the other cores. In comparison to cores 23-GC1 and 24-GC1, there is also a slight increase in garnet content in core 29-GC1. Core 20-GC1 has the highest titanite, zircon and ilmenite content.

https://doi.org/10.5194/cp-2021-111
Preprint. Discussion started: 7 September 2021

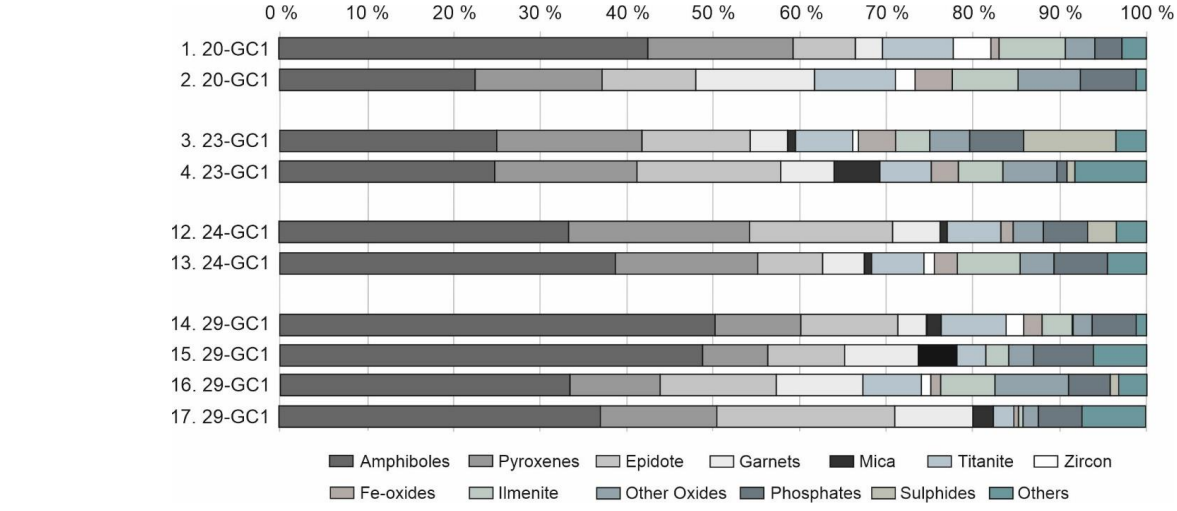

Figure 4: The distribution of heavy minerals of diamict and deglacial sediments of samples studied. Samples 1 and 2 are deglacial sediments from the East Siberian shelf and their deposition correlate to the sediments from the last glacial cycle in the upper part of cores 23-GC1 and 24-GC1. Samples 3, 4, 12, and 13 are diamict from the base of cores 23-GC1 and 24-GC1 from the De Long Trough. Sample 14 is deglacial clay and samples 15–17 are diamict from the base of core 29-GC1 from the southern Lomonosov Ridge.

From core 24-GC1 five samples (5, 6, 9, 10, and 11) of surface sediments and other lithologies overlying the diamicts were selected to compare the heavy mineral assemblages with the underlying diamicts (12 and 13) and to detect possible stratigraphic variability in heavy mineral assemblages along the core (Fig. 5). Two of the treated samples (7 and 8) did not have enough coarse fraction grains or heavy minerals to be analyzed. As an additional note, the heavy mineral grain content in samples 5 and 11 is notably lower (n = 24-36) than in the other samples. The diamicts from samples 12 and 13 consist mostly of amphiboles (33–39%), pyroxenes (17–21%), and epidote (7–17%), with minor mineral composition ranging between 1 and 7%. In comparison to these diamicts, in the interglacial sediment samples there is less amphiboles (8–28%), varying amount of pyroxenes (6–23%), and epidote (8–20%). There is a notable increase of garnet content in sample 11, and it is the most abundant mineral in the sample. Although minor minerals are present in the assemblages, varying from 1 to 11%, there appears peaks in concentrations of other heavy minerals (incl. chlorite) in sample 5 (19%) and phosphates in sample 10 (14%). Overall, the amphibole content is higher in the diamicts (up to 39%) than in the interglacial sediments (up to 28%). The pyroxene concentration is smaller and fluctuates more in the interglacial sediments than in the diamicts. Epidote concentration is similar in the diamicts and overlying sediments. Minor minerals are slightly more abundant in the interglacial sediments than in the diamicts, in addition to the previously mentioned peaks in samples 5 and 10. The overlying interglacial sediments show an increase in iron oxide content right above the diamict and in the uppermost part of the core. There is also an increase in other oxides in the middle part of the core, and in titanite content upwards from the middle part of the core.

https://doi.org/10.5194/cp-2021-111
Preprint. Discussion started: 7 September 2021

Climate of the Past Discussions

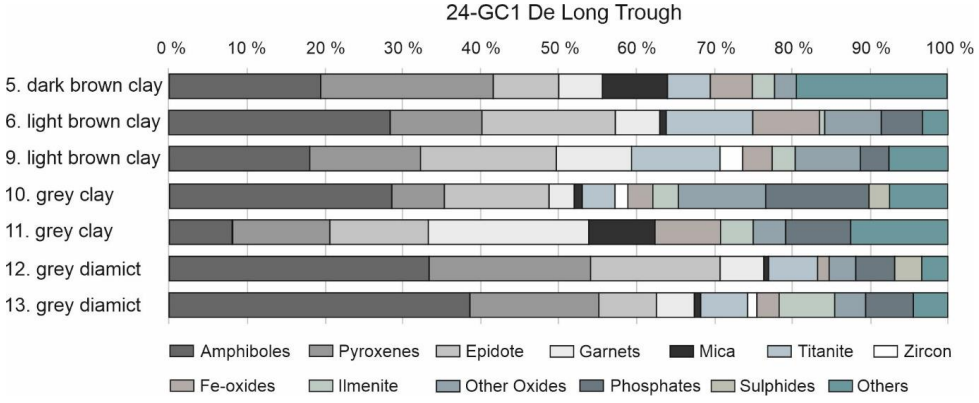

Figure 5: The distribution of heavy minerals of sediments from core 24-GC1 from the De Long Trough. Samples 12 and 13 are grey diamict from the base of the core. Samples 9, 10 and 11 are interglacial sediments from the middle part of the core, and samples 5 and 6 are from the upper part of the core above the radiocarbon age point of 43 000 ±1800 ^{14}C years BP.

5 Discussion

This provenance study contributes in outlining the glacial history of the ESS and shelf area and demonstrates interpretation of parent rocks and sediment source areas. Parent rocks determine the basics for heavy mineral assemblages, and since sedimentary processes are governed by glacial ice dynamics, it can be assumed that changes in mineralogy reflect also changes in sediment sources and ice streaming before final deposition and burial. The distribution of heavy minerals in the sediments is influenced by the differention between sub-ice and subglacial shelf, and open-marine sedimentary processes.

5.1 Parent rocks for heavy minerals

The heavy mineral assemblages can be used to define possible parent rocks and provide insights into the overall sediment provenance and transport history in cases when reworking and mixing of several sources have occurred before deposition. The heavy minerals from cores 20-GC1, 23-GC1, 24-GC1 and 29-GC1 were interpreted by considering diverse sediment transport pathways e.g. major river transport as well as parent rocks in hinterland. In this study the heavy mineral assemblages were compared with published data from eastern Siberian geological provinces (Fig. 6) and their major rocks and heavy minerals (Table 3). According to this comparison and a closer look at the geochemical compositions of individual heavy minerals, it is possible to identify the main parent rocks for DLT sediments and the studied southern LR sediments. The geology of the hinterland areas is characterized by the Archean and Paleoproterozoic Shield Complex called the Omolon massif, Paleozoic–Mesozoic orogenic fold belts including the Chukotka Fold Belt (CFB) and the Verkhoyansk Fold Belt (VFB), Mesozoic–Cenozoic Okhotsk–Chukotka Volcanic Belt (OCVB) and related sedimentary rocks, and Paleozoic–Mesozoic platforms as well as the ESS sediments. The VFB along with CFB are major metamorphic sources. According to Prokopiev et al. (2009) Early to Middle Paleozoic carbonate and terrigenous rocks are predominantly actinolite-chlorite, sericite-chlorite, epidote-actinolite-chlorite, and carbonate-sericite-chlorite-quartz-albite schists in their present metamorphic form. The OCVB can be considered as a major igneous and volcanic source. It includes Paleozoic–Late Cretaceous granitoids and gabbroic intrusions and Early Jurassic–Late Cretaceous basaltic andesites and rhyolite tuffs and ignimbrites (Kabanova et al. 2011). Tikhomirov et al. (2012) divided the stratigraphy of the OCVB into three main components as follows; the lower andesites, the group of formations dominated by silicic rocks and the upper basalts.

https://doi.org/10.5194/cp-2021-111
Preprint. Discussion started: 7 September 2021

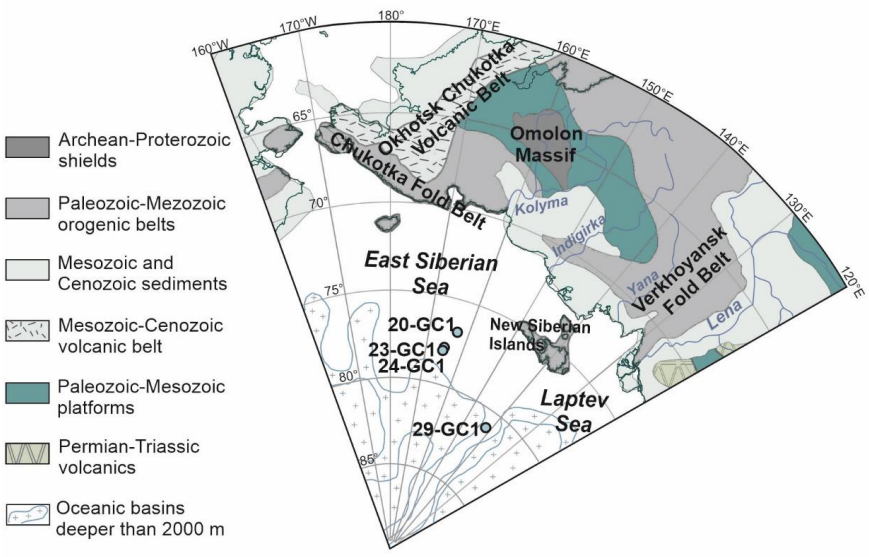

Figure 6: Main geological structures of the probable provenance areas for the studied sediments. Adapted from Stein (2008) and Kaparulina et al. (2016).

Table 3: Summary of lithological and mineralogical characteristics of the hinterland area for the De Long Trough and southern Lomonosov Ridge sediments.

Geological province or area	Geology and lithologies of source rocks	Heavy minerals
Omolon Massif [1,2,3]	Archaean and Proterozoic magmatic and metamorphic rocks; granulites (high grade metamorphic rocks), gneisses, quartzites, and granites	Major: garnet, amphiboles (hornblende), hypersthene Minor: magnetite, sapphirine-spinel
Verkhoyansk Fold Belt4 [4,5,6]	Paleozoic shales and carbonate rocks, Mesozoic sand-siltstones and black shales (mid- to low-grade metamorphic rocks)	Major: amphiboles (hornblende, actinolite), garnet, Fe-oxides Minor: dolomite, epidote
Chukotka Fold Belt [7,8]	Paleozoic shales and carbonate rocks, Mesozoic sand-siltstones, and shales, some granitoids (mid- to low-grade metamorphic rocks); Triassic gabbroic rocks, some Cretaceous volcanogenic rocks	Major: amphiboles (hornblende, actinolite), biotite, apatite, Minor: sillimanite, andalusite, sphene, zircon
Siberian platform [9]	Paleozoic–Mesozoic volcanic–sedimentary rocks; Jurassic sand-siltstones and tuffaceous rocks	Major: Fe-oxides, pyroxenes, hornblende Minor: zircon
Okhotsk-Chukotka Volcanic Belt [10, 11, 12, 13, 14]	Paleozoic-Early Mesozoic sandstones, Paleozoic-Late Cretaceous granitoid and gabbroic rocks, Early Jurassic-Late Cretaceous calc-alkaline volcanic rocks, and felsic ignimbrites	Major: pyroxenes, amphiboles, garnet, epidote, biotite Minor: magnetite, ilmenite, apatite, sphene, zircon, olivine, monazite
East Siberian Sea [15, 16]	Silty-clay, clayey-silt, sandy-silty-clay associated with ice drafting. Sources of the sediments of the East Siberian Sea are the Indigirka and Kolyma rivers and the New Siberian Island region. Central plateau is characterized by low concentrations of heavy minerals.	Major: amphiboles (hornblende, actinolite) pyroxenes, Fe-oxides, ilmenite, biotite, epidote Minor: zircon, sphene, anatase, rutile

References: 1) Akinin and Zhulanova (2016), 2) Avchenko and Chudnenko (2020), 3) Drachev (2016), 4) Kaparulina et al. (2016), 5) Konstaninovsky (2007), 6) Prokopiev et al. (2009), 7) Miller et al. (2009), 8) Katkov et al. (2007), 9) Filatova and Khain (2008), 10) Akinin and Miller (2011), 11) Belyi (1977), 12) Kabanova et al. (2011), 13) Tikhomirov et al. (2012), 14) Tschegg et al. (2011), 15) Naugler et al (1974), 16) Nikolaeva et al. (2013).

5.2 The glacial and interglacial transitions

The surface sediments and other lithologies overlying the diamicts from core 24-GC1 enable also the consideration of stratigraphic variability in heavy mineral assemblages along the core (Fig. 5). It can be assumed that changes in mineralogy between the diamicts and the overlying interglacial/interstadial sediments in the DLT reflect those changes related to dynamics of the deglaciation in the ESS. The layer of olive green/grey fine grained sediments in core 24-GC1 are characterized by the

https://doi.org/10.5194/cp-2021-111
Preprint. Discussion started: 7 September 2021

Climate of the Past Discussions

lack of grain size > 63 µm and the studied samples from this part of the core retrieved no heavy minerals. The sediments were possibly derived from the central plateau of the ESS which is characterized by low concentrations of heavy minerals (cf. Naugler et al., 1974). These factors indicate that during the deposition of these sediments the central plateau or at least the shoreline and river discharge region was possibly free from ice, or the ice sheet was relatively thin and not grounding on the plateau. These sediments also show a slight increase in Fe-oxides content which indicates sea-ice rather than iceberg transport. Transitions from glacial to interglacial conditions are documented in core 24-GC1 (at ca. 3.6 m b.s.f.) by a shift from diamict-dominated sediments to interglacial clay dominated sediments. Although, these diamicts are intepreted as deposited most likely during glacial period of MIS 6, deposition during a stadial in MIS 5 or the glacial period of MIS 4 is possible. The finer-grained, grey sediments just above the diamicts are most likely related to glacial maxima and followed by deglacial deposition.

5.3 Consideration of the heavy mineral assemblages for the ESIS distribution

During glaciations sediments at the East Siberian shelf and slope were fed by grounded ice and major rivers which delivered detritus from the eastern hinterland regions. The diamicts were deposited from glacial ice that collected debris predominantly by eroding the continental shelf. When open marine conditions prevailed, sediments from local sources were provided. The primary riverine sources for the ESS sediments are the Indigirka and Kolyma rivers (e.g. Naugler et al., 1974). These sediments are also a major contributor in materials eroded and re-deposited by glacial ice in the DLT. The heavy mineral assemblages of sediments occupied in paleovalley of the Indigirka river have higher abundances of amphiboles with relatively high proportions of titanite and ilmenite, in comparison to the Kolyma river paleovalley sediments which show a higher share of pyroxenes and epidote (cf. Nikolaeva et al., 2013). These are comparable with our heavy mineral assemblages (Figs. 4 and 5). A distinct feature in these assemblages is the elevated content of minerals characteristic of ancient volcanogenic and volcanogenic-sedimentary rocks of greenstone metamorphism enriched in amphibole, pyroxenes and epidote. Higher amounts of ilmenite and magnetite are interpreted as possible indicators of erosional processes in shallow-water environments (cf. Stein, 2008). Assemblages with elevated amphibole and garnet content, along with higher titanite, ilmenite, and other oxides content in sediments from core 29-GC1 from the southern LR are most likely delivered from the VFB and westerly sources. Fold belts are usually metamorphosed provinces indicative for medium to high-grade facies rocks and minerals such as actinolites, hornblendes, kyanite, and garnets. The mineralogical signature of the DLT diamicts consisting predominantly of amphiboles and pyroxenes with minor content of garnet and epidote, show a clear delivery from the eastern sector of the ESIS. The physical properties of the DLT basal diamict closely resemble a pervasive diamict unit recovered across the southern LR off Siberia, but according to their heavy mineral content their source material is slightly different. The assemblages from core 29-GC1 from the southern LR have elevated amphibole and garnet content, along with higher titanite and ilmenite content, which emphasise the VFB as a possible source. This suggests that glacial ice not only grew out from the East Siberian shelf but also from the New Siberian Islands and westerly sources due to dynamics in ice flow and deposition. Glacial deposits on the New Siberian Islands (Nikolskiy et al., 2017), and the orientation of glaciogenic features on the northeastern Siberian continental shelf (Jakobsson et al., 2016), along with the glacially scoured DLT offer further evidence for the wider extent of ESIS. Ice streams occupying the DLT likely fed into the massive ice shelf complex that scoured the southern and central LR (Jakobsson et al., 2016). O'Regan et al. (2017) concluded that orientation of glacio-tectonic features illustrate that glacial ice flowed from a north-northeast direction on the New Siberian Islands and likely nucleated and extended over the De Long Islands. It is suggested that there was an extensive ice sheet in the northeastern Siberia particularly during MIS 6 (Colleoni et al., 2016; Jakobsson et al., 2016; Wekerle et al., 2016; Nikolskiy et al., 2017) and further supported by this study.

https://doi.org/10.5194/cp-2021-111
Preprint. Discussion started: 7 September 2021

Climate of the Past Discussions

6 Conclusions

The data from the heavy mineral analysis and interpretations presented here provide new insights that sediments delivered to the East Siberian shelf by the Indigirka and Kolyma river, are a primary source for sediments eroded and re-deposited by glacial ice in the De Long Trough (DLT). Mineralogical signature of the diamicts from the DLT consists predominantly of amphiboles and pyroxenes with minor content of garnet and epidote and illustrate a clear delivery from the eastern sector of the East Siberian Ice Sheet. The physical properties of the DLT basal diamict closely resemble a pervasive diamict unit recovered from the southern Lomonosov Ridge (LR), but the heavy mineral content indicate slightly different source material. Assemblages with elevated amphibole and garnet content, along with higher titanite and ilmenite content from core 29-GC1 from the southern LR accentuate the Verkhoyansk Fold Belt as a possible source area. This suggests that due to dynamics of the ice flow and deposition the glacial ice not only grew out from the East Siberian shelf but also from the New Siberian Islands and westerly sources. Increased iron oxides content in the sediments overlying the diamicts is related to the deglaciation cycle of the ESIS when the central plateau, or at least the shoreline and river discharge region, were possibly free from ice, and the reworking as well as enrichment of iron oxides was possible. This is an indication of sea-ice rather than iceberg transport of the present distal shelf sediments.

Author contribution

Raisa Alatarvas did the laboratory work and SEM analysis and produced the figures and tables. Raisa Alatarvas prepared and wrote the manuscript with contributions from all co-authors. Matthew O'Regan provided the samples.

Competing interests

The authors declare that they have no conflict of interest.

Acknowledgements

We thank the supporting crew and Captain of I/B Oden and the support of the Swedish Polar Research Secretariat for realizing the cruise and coring operations. This research is part of the University of Oulu funded project Loss of Ice in the Arctic System (LIAS): geological perspective of global environmental change. This research was partially supported by the Finnish Cultural Foundation. Many thanks to Riitta Kontio from the Oulu Mining School Research Center for laboratory assistance. Special thanks to Leena Palmu and Pasi Juntunen from the Centre for Material Analysis (CMA) at the University of Oulu for assistance with SEM.

References

Akinin, V.V. and Miller, E.L.: Evolution of Calc-Alkaline Magmas of the Okhotsk–Chukotka Volcanic Belt, Petrology, Vol. 19, No. 3, pp. 237–27, https://doi.org/10.1134/S0869591111020020, 2011.

Akinin, V.V., and Zhulanova, L.L.: Age and geochemistry of zircon from the oldest metamorphic rocks of the Omolon Massif (Northeast Russia), Geochemistry International, Vol. 54, No. 8, pp. 651–659, https://doi.org/10.1134/S0016702916060021, 2016.

Avchenko, O.V. and Chudnenko, K.V.: The Probable Metapelite Nature of Sapphirine–Spinel and Garnet Gedritites of the Aulandzha Block of the Omolon Massif, Russian Geology and Geophysics, 61, 7, 689–699, https://doi.org/10.15372/RGG2019157, 2020.

Backman, J., Fornaciari, E., and Rio, D.: Biochronology and paleoceanography of late Pleistocene and Holocene calcareous nannofossil abundances across the Arctic Basin, Mar. Micropaleontol., 72, 86–98, https://doi.org/10.1016/j.marmicro.2009.04.001, 2009.

Basilyan, A., Nikol'skyi, P., and Anisimov, M.: Pleistocene glaciation of the New Siberian Islands - no more doubt, IPY News, 12, 7–9, 2008.

Batchelor, C. L. and Dowdeswell, J. A.: The physiography of High Arctic cross-shelf troughs, Quaternary Sci. Rev., 92, 68–96, https://doi.org/10.1016/j.quascirev.2013.05.025, 2014.

https://doi.org/10.5194/cp-2021-111
Preprint. Discussion started: 7 September 2021

Belyi, V.F.: *Stratigrafiya i struktury Okhotsko–Chukotskogo vulkanogennego poyasa* (Stratigraphy and Structures of the OkhotskMChukotka Volcanogenic Belt), Moscow: Nauka, 1977.

Cochran, J.R., Edwards, M.H., and Coakley B.J.: Morphology and structure of the Lomonosov Ridge, Arctic Ocean, Geochemistry, Geophysics, Geosystems, 7, 5, https://doi.org/10.1029/2005GC001114, 2006.

Colleoni, F., Kirchner, N., Niessen, F., Quiquet, A., and Liakka, J.: An East Siberian ice shelf during the Late Pleistocene glaciations: Numerical reconstructions, Quaternary Sci. Rev., 147, 148–163, https://doi.org/10.1016/j.quascirev.2015.12.023, 2016.

Cronin, T.M., O'Regan, M., Pearce, C., Gemery, L., Toomey, M., Semiletov, I., Jakobsson, M.: Deglacial sea level history of the East Siberian Sea and Chukchi Sea margins. Clim. Past, 13, 1097–1110, https://doi.org/10.5194/cp-13-1097-2017, 2017.

Drachev, S.S., Malyshev, N.A., and Nikishin, A.M.: Tectonic history and petroleum geology of the Russian Arctic Shelves: an overview, Petroleum Geology Conference series, v. 7, p. 591–619, https://doi.org/10.1144/0070591, 2010.

Drachev, S.: Fold belts and sedimentary basins of the Eurasian Arctic, Arktos, 2:21, https://doi.org/10.1007/s41063-015-0014-8, 2016.

Drachev, S.S., Mazur, S., Campbell, S., Green, C., and Tishchenko, A.: Crustal architecture of the East Siberian Arctic Shelf and adjacent Arctic Ocean constrained by seismic data and gravity modelling results, Journal of Geodynamics, 119, pp. 123–148, https://doi.org/10.1016/j.jog.2018.03.005, 2018.

Dowdeswell, J.A., and Ó Cofaigh, C. (eds): Glacier-influenced Sedimentation on High-Latitude Continental Margins: introduction and overview, Geological Society, London, Special Publications, 203, 1–9, https://doi.org/10.1144/GSL.SP.2002.203.01.01, 2002.

Dowdeswell, J.A., Canals, M., Jakobsson, M., Todd, B.J., Dowdeswell, E.K., and Hogan, K.A.: The variety and distribution of submarine glacial landforms and implications for ice-sheet reconstruction, Geological Society, London, Memoirs, 46, 519–552, https://doi.org/10.1144/M46.183, 2016.

Elverhøi, A., Norem, H., Andersen, E. S., Dowdeswell, J. A., Fossen, I., Haflidason, H., Kenyon, N. H., Laberg, J. S., King, E. L., Sejrup, H. P., Solheim, A., and Vorren, T.: On the origin and flow behaviour of submarine slides on deep-sea fans along the Norwegian–Barents Sea continental margin, Geo-Marine Letters, 17, 119–125, https://doi.org/10.1007/s003670050016, 1997.

Filatova, N.I., and Khain, V.E.: Development of the Verkhoyansk–Kolyma Orogenic System As a Result of Interaction of Adjacent Continental and Oceanic Plates, Geotectonics, Vol. 42, No. 4, pp. 258–285, https://doi.org/10.1134/S001685210804002X, 2008.

Jakobsson, M., Nilsson, J., O'Regan, M., Backman, J., Löwemark, L., Dowdeswell, J.A., Mayer, L., Polyak, L., Colleoni, F., Anderson, L.G., Björk, G., Darby, D., Eriksson, B., Hanslik, D., Hell, B., Marcussen, C., Sellén E., and Wallin, Å.: An Arctic Ocean ice shelf during MIS 6 constrained by new geophysical and geological data, Quaternary Science Reviews, 29, 3505–3517, https://doi.org/10.1016/j.quascirev.2010.03.015, 2010.

Jakobsson, M., Mayer, L.A., Coakley, B., Dowdeswell, J.A., Forbes, S., Fridman, B., Hodnesdal, H., Noormets, R., Pedersen, R., Rebesco, M., Schenke, H-W., Zarayskaya, Y., Accettella, A.D., Armstrong, A., Anderson, R.M., Bienhoff, P., Camerlenghi, A., Church, I., Edwards, M., Gardner, J.V., Hall, J.K., Hell, B., Hestvik, O.B., Kristoffersen, Y., Marcussen, C., Mohammad, R., Mosher, D., Nghiem, S.V., Pedrosa, M.T., Travaglini, P.G., and Weatherall, P.: The International Bathymetric Chart of the Arctic Ocean (IBCAO) Version 3.0, Geophysical Research Letters, doi: 10.1029/2012GL052219, 2012.

Jakobsson, M., Andreassen, K., Bjarnadóttir, L. R., Dove, D., Dowdeswell, J. A., England, J. H., Funder, S., Hogan, K., Ingólfsson, Ó., Jennings, A., Larsen, N. K., Kirchner, N., Landvik, J. Y., Mayer, L., Mikkelsen, N., Möller, P., Niessen, F., Nilsson, J., O'Regan, M., Polyak, L., Nørgaard-Pedersen, N., and Stein, R.: Arctic Ocean glacial history, Quaternary Sci. Rev., 92, 40–67, https://doi.org/10.1016/j.quascirev.2013.07.033, 2014.

Jakobsson, M., Nilsson, J., Anderson, L., Backman, J., Björk, G., Cronin, T.M., Kirchner, N., Koshurnikov, A., Mayer, L., Noormets, R., O'Regan, M., Stranne, C., Ananiev, R., Barrientos Macho, N., Cherniykh, D., Coxall, H., Eriksson, B., Flodén, T., Gemery, L., Gustafsson, Ö., Jerram, K., Johansson, C., Khortov, A., Mohammad, R., Semiletov, I.: Evidence for an ice shelf covering the central Arctic Ocean during the penultimate glaciation, Nature Communications 7, 10365, https://doi.org/10.1038/ncomms10365, 2016.

Jokat, W., and Ickrath, M.: Structure of ridges and basins off East Siberia along 81°N, Arctic Ocean, Marine and Petroleum Geology, 64, 222–232, http://dx.doi.org/10.1016/j.marpetgeo.2015.02.047, 2015.

Kabanova, O.I., Tikhomirov, P.L., and Yapaskurt, V.O.: Phenocrysts in Silicic Volcanic Rocks in the Northern Part of the Okhotsk–Chukotka Belt and Their Crystallization Conditions, Petrology, Vol. 19, No. 3, pp. 278–296, https://doi.org/10.1134/S0869591111030040, 2011.

Kaparulina, E., Strand, K., and Lunkka, J.P.: Provenance analysis of central Arctic Ocean sediments: Implications for circum-Arctic ice sheet dynamics and ocean circulation during Late Pleistocene, Quaternary Science Reviews, 147, 210–220, http://dx.doi.org/10.1016/j.quascirev.2015.09.017, 2016.

Katkov, S.M., Strickland, A., Miller, E.L., and Toro, J.: Age of Granite Batholiths in the Anyui–Chukotka Foldbelt, Doklady Earth Sciences, Vol. 414, No. 4, pp. 515–518, https://doi.org/10.1134/S1028334X07040058, 2007.

Klemann, V., Heim, B., Bauch, H.A., Wetterich, S., Opel, T: Sea-level evolution of the Laptev Sea and the East Siberian Sea since the last glacial maximum, Arktos, 1, 1, https://doi.org/10.1007/s41063-015-0004-x, 2015.

Kristoffersen, Y.: Eurasia Basin, The Geology of North America, 50, 365–378, https://doi.org/10.1130/DNAG-GNA-L.365, 1990.

https://doi.org/10.5194/cp-2021-111
Preprint. Discussion started: 7 September 2021

Laberg, J. S. and Vorren, T. O.: Late Weichselian submarine debris flow deposits on the Bear Island Trough Mouth Fan, Mar. Geol., 127, 45–72, https://doi.org/10.1016/0025-3227(95)00055-4, 1995.

Lambeck, K., Rouby, H., Purcell, A., Sun, Y., and Sambridge, M.: Sea level and global ice volumes from the Last Glacial Maximum to the Holocene, P. Natl. Acad. Sci. USA, 111, 15296–15303, https://doi.org/10.1073/pnas.1411762111, 2014.

Licht, K.J. and Hemming, S.R.: Analysis of Antarctic glacigenic sediment provenance trough geochemical and petrologic applications, Quaternary Science Reviews, 164, 1–24, 2017.

Mange, M.A., Maurer, F.W.: Heavy minerals in Colour. Chapman & Hall, London, 1992.

Miller, E.L., Katkov, S.M., Strickland, A., Toro, J., Akini, V.V., and Dumitru, T.A.: Geochronology and thermochronology of Cretaceous plutons and metamorphic country rocks, Anyui-Chukotka fold belt, North East Arctic Russia, Stephan Mueller Spec. Publ. Ser., 4, 157–175, https://doi.org/10.5194/smsps-4-157-2009, 2009.

Naugler, F.P., Silverberg, N., and Creager, J.S.: Recent Sediments of the East Siberian Sea, In: Herman, Y., (eds.) Marine Geology and Oceanography of the Arctic Seas, Springer, Berlin, Heidelberg, pp. 191–210, https://doi.org/10.1007/978-3-642-87411-6, 1974.

Niessen, F., Hong, J. K., Hegewald, A., Matthiessen, J., Stein, R., Kim, H., Kim, S., Jensen, L., Jokat, W., and Nam, S.: Repeated Pleistocene glaciation of the East Siberian continental margin, Nature Geosci., 6, 842–846, https://doi.org/10.1038/ngeo1904, 2013.

Nikolaeva, N.A., Derkachev, A.N., and Dudarev, O.V.: Mineral composition of sediments from the Eastern Laptev Sea shelf and East Siberian Sea, Oceanology, Vol. 53, No. 4, pp. 472–480, https://doi.org/10.1134/S0001437013040073, 2013.

Nikolskiy, P.A., Basilyan, A.E., and Zazhigin, V.S.: New Data on the Age of the Glaciation in the New Siberian Islands (Russian Eastern Arctic), Doklady Earth Sciences, 475, 1, pp. 748–752, DOI: 10.1134/S1028334X17070194, 2017.

Ó Cofaigh, C., Taylor, J., Dowdeswell, J. A., and Pudsey, C. J.: Palaeo-ice streams, trough mouth fans and high-latitude continental slope sedimentation, Boreas, 32, 37–55, https://doi.org/10.1080/03009480310001858, 2003.

O'Regan, M., Preto, P., Stranne, C., Jakobsson, M., Koshurnikov, A.: Surface heat flow measurements from the East Siberian continental slope southern Lomonosov Ridge, Arctic Ocean, Geochemistry, Geophysics, Geosystems, 17, 5, https://doi.org/10.1002/2016GC006284, 2016.

O'Regan, M., Backman, J., Barrientos, N., Cronin, T.M., Gemery, L., Kirchner, N., Mayer, L.A., Nilsson, J., Noormets, R., Pearce, C., Semiletov, I., Stranne, C., Jakobsson, M.: The De Long Trough: a newly discovered glacial trough on the East Siberian continental margin. Climate of the Past, 13, 1269–1284, https://doi.org/10.5194/cp-13-1269-2017, 2017.

O'Regan, M., Backman, J., Fornaciari, E., Jakobsson, M., and West, G.: Calcareous nannofossils anchor chronologies for Arctic Ocean sediments back to 500 ka. Geology, 48 (11), p. 1115–1119. http://doi.org/10.1130/G47479.1, 2020.

Prokopiev, A.V., Toro, J., Hourigan, J.K., Bakharev, A.G., and Miller, E.L.: Middle Paleozoic-Mesozoic boundary of the North Asian craton and the Okhotsk terrane: new geochemical and geochronological data and their geodynamic interpretation, Stephan Mueller Spec. Publ. Ser., 4, 71–84, https://doi.org/10.5194/smsps-4-71-2009, 2009.

Rohling, E. J., Foster, G. L., Grant, K.M, Marina, G., Roberts, A.P., Tamisiea, M. E., and Williams, F.: Sea-level and deep-seatemperature variability over the past 5.3 million years, Nature, 508, 477–482, https://doi.org/10.1038/nature13230, 2014.

Stein, R., Boucsein, B., Fahl, K., Garcia de Oteyza, T., Knies, J., and Niessen, J.: Accumulation of particulate organic carbon at the Eurasian continental margin during late Quaternary times: controlling mechanisms and paleoenvironmental significance, Global and Planetary Change, 31, 87–104, https://doi.org/10.1016/S0921-8181(01)00114-X, 2001.

Stein, R.: Arctic Ocean sediments: processes, proxies, and paleoenvironment, In: Chamley, H. (Ed.), Dev. In Mar. Geo, 2. Elsevier, p. 587, 2008.

SWERUS Scientific Party: Cruise Report SWERUS-C3 Leg 2, Bolin Centre for Climate Research, No 2, 2014.

Tikhomirov, P.L., Kalinina, E.A., Moriguti, T., Makishima, A., Kobayashi, K., Cherepanova, I.Yu., and Nakamura, E.: The Cretaceous Okhotsk–Chukotka Volcanic Belt (NE Russia): Geology, geochronology, magma output rates, and implocations on the genesis of silicic LIPs, Journal of Volcanology and Geothermal Research, 221–222, 14–32, https://doi.org/10.1016/j.jvolgeores.2011.12.011, 2012.

Tschegg, C., Ntaflos, T., and Akinin, V.V.: Polybaric petrogenesis of Neogene alkaline magmas in an extensional tectonic environment: Viliga Volcanic Field, northeast Russia, Lithos, 122, 13–24, https://doi.org/10.1016/j.lithos.2010.11.009, 2011.

Wekerle, C., Colleoni, F., Näslund, J.-O., Brandfelt, J., and Masina, S.: Numerical reconstructions of the penultimate glacial maximum Northern Hemisphere ice sheets: sensitivity to climate forcing and model paremeters, Journal of Glaciology, 62, 234, pp. 607–622, https://doi.org/10.1017/jog.2016.45, 2016.